The Ferroxidase Centre of *Escherichia coli* Bacterioferritin Plays a Key Role in the Reductive Mobilisation of the Mineral Iron Core

Justin M. Bradley[1], Zinnia Bugg[1], Aaren Sackey[1], Simon C. Andrews[2], Michael T. Wilson[3], Dimitri A. Svistunenko[3], Geoffrey R. Moore[1] and Nick E. Le Brun[1]

[1]Centre for Molecular and Structural Biochemistry, School of Chemistry, University of East Anglia, Norwich Research Park, Norwich, NR4 7TJ, UK
[2]School of Biological Sciences, University of Reading, Whiteknights, Reading, RG6 6AS
[3]School of Life Sciences, University of Essex, Wivenhoe Park, Colchester, CO4 3SQ

Correspondence: Justin M. Bradley (justin.bradley@uea.ac.uk) and Nick E. Le Brun (n.le-brun@uea.ac.uk)

Keywords
Electron transfer, iron, heme, ferritin, iron homeostasis, magnetic circular dichroism

Graphical Abstract

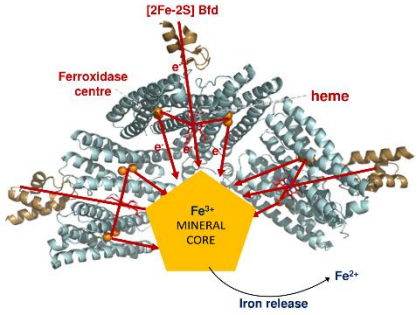

The diiron ferroxidase centres of ferritins are required for Fe^{2+} oxidation and formation of the mineral core. Here, we show that the ferroxidase centres of bacterioferritin (Bfr) also play a key role in iron release, and that this is dependent on electron transfer from the Bfr heme to the ferroxidase centre.

Abstract
Ferritins are multimeric cage-forming proteins that play a crucial role in cellular iron homeostasis. All H-chain-type ferritins harbour a diiron site, the ferroxidase centre, at the centre of a 4 α–helical bundle, but bacterioferritins are unique in also binding 12 hemes per 24meric assembly. The ferroxidase centre is known to be required for the rapid oxidation of Fe^{2+} during deposition of an immobilised ferric mineral core within the protein's hollow interior. In contrast, the heme of bacterioferritin is required for the efficient reduction of the mineral core during iron release, but has little effect on the rate of either oxidation or mineralisation of iron. Thus, the current view is that these two cofactors function in iron uptake and release, respectively, with no functional overlap. However, rapid electron transfer between the heme and ferroxidase centre of bacterioferritin from *Escherichia coli* was recently demonstrated, suggesting that the two cofactors may be functionally connected. Here we report absorbance and (magnetic) circular dichroism spectroscopies, together with *in vitro* assays of iron-release kinetics, which demonstrate that the ferroxidase centre plays an important role in the reductive mobilisation of the bacterioferritin mineral core, which is dependent on the heme-ferroxidase centre electron transfer pathway.

Introduction
The redox chemistry of iron is ideally suited to supporting many essential biological processes, with Fe^{2+}, Fe^{3+} and Fe^{4+} oxidation states all within the accessible intracellular range of electrochemical potential and the midpoint potentials that characterise their interconversion readily tunable by the coordination environment of the metal[1]. Prior to the oxygenation of the atmosphere, iron was readily available as soluble Fe^{2+} and as a result early terrestrial life evolved to be reliant upon it[2]. Consequently the great oxidation event of the paleoprotozoic era presented a dual challenge to living systems. Combination of iron and O_2 led to the formation of insoluble mineral deposits such as haemetite, greatly limiting the availability of iron, such that it is now commonly a growth-limiting nutrient in aerobic environments. Furthermore, the facile transition between the Fe^{2+} and Fe^{3+} oxidation states catalyses the formation of damaging reactive oxygen species (ROS), particularly hydroxyl radicals, from the byproducts of aerobic respiration[3]. Therefore the intracellular concentration of chelatable iron, the labile iron pool, is tightly regulated in order to ensure correct metallation of the iron containing proteome whilst also limiting the potential for iron-induced oxidative stress[4].

Ferritins play a crucial role in cellular iron homeostasis by providing a chemically inert store of this often hard to come by micronutrient when it is present above metobolic requirements. This store of ferrihydrite-like mineral can then be drawn on in times of iron limitation[5]. Their importance in managing iron status and oxidative stress is such that examples are widespread in all kingdoms of life[6]. The majority of the cage-forming members of the ferritin superfamily assemble into rhombic dodecahedra in which each of the 12 faces is composed of a subunit dimer[7], the notable exception being the dodecameric Dps-like proteins found only in prokaryotes[8]. Despite the often low sequence identity between different classes of ferritin, the protomers of the 24meric examples are isostructural and can therefore co-assemble into heteropolymers surrounding an internal cavity of 80 Å diameter[9]. It has long been known that animal ferritins located in the cytosol form heteropolymers[10] with tissue specific ratios of H-chains that contain diiron catalytic ferroxidase centres[11], and L-chains that lack ferroxidase centres but

initiate the formation of the mineral core from nucleation sites located on their inner surface[12]. In contrast, prokaryotic genomes often encode several ferritins that belong to three classes[4], the H-chain-like Ftns, Dps proteins and bacterioferritins (Bfrs). The defining characteristics of the Bfrs are a unique ferroxidase centre architecture, similar to that of the diiron site in the class I RNRs[13], together with a heme cofactor at the interface of each of the dimeric faces with the sulfur atom of a conserved methionine in each protomer providing the axial ligands to the heme iron[14]. Prokaryotic ferritins were originally thought to assemble into homopolymers but recent evidence suggests that, whilst homopolymers are formed *in vivo* under certain conditions, when Ftns and Bfrs are expressed simultaneously they may also co-assemble to form heteropolymers[15].

The majority of studies of ferritins have focussed on the mechanism of catalytic oxidation of Fe^{2+} at the ferroxidase centre and the subsequent formation of an Fe^{3+}-containing mineral core. These have revealed mechanistic variation between ferritins that reflect variation in primary cellular role between iron storage and antioxidant activity[16]. This is illustrated by comparison between the Bfrs of *Pseudomonas aeruginosa* and *Escherichia coli*. The former functions as the primary source of stored iron and its ferroxidase centres act as catalytic sites where Fe^{2+} binds, is oxidised by either O_2 or peroxide and the Fe^{3+} product released into the internal cavity, regenerating apo sites able to bind and oxidise further equivalents of Fe^{2+} substrate[17]. The role of the *E. coli* protein is thought to be peroxide detoxification and alleviation of oxidative stress, and the ferroxidase centre has been shown to act as a cofactor, binding Fe^{2+} that, following an initial oxidation step, cycles between the Fe^{3+} and Fe^{2+} states to facilitate the transfer of electrons from Fe^{2+} located within the internal cavity to O_2 or peroxide bound at the ferroxidase centre to drive mineral formation[18].

Mechanistic understanding of the release of iron from ferritins is poor in comparison to iron oxidation and storage. The notable exception to this is the bacterioferritins, where the fractional occupancy of the heme binding site has been demonstrated to affect the rate of iron release mediated by exogenous reductants[19]. Bacterial genomes very often contain a gene, located upstream of the *bfr* gene, encoding a small (approximately 60 residues) ferredoxin. These bacterioferritin-associated ferredoxins (Bfds) have been shown to bind to Bfr[20], with the [2Fe-2S] cluster of the ferredoxin ideally situated to transfer electrons to the heme of the ferritin (Fig. 1). Consequently, Bfd was proposed to provide a conduit for electron transfer from sources such as NADPH, via a ferredoxin reductase, to the heme of Bfr and ultimately the ferrihydrite-like mineral core to initiate reduction to soluble Fe^{2+} that can be recovered from the interior of the ferritin under conditions of iron deficiency. Indeed, in *P. aeruginosa* where Bfr constitutes the primary iron-storage protein, disruption of the Bfr-Bfd interface leads to irreversible accumulation of iron within the ferritin cage with consequent depletion of cytoplasmic iron[21]. Small molecules targeting the Bfr-Bfd interaction have been shown to lead to reduced cell viability, even in biofilms that are tolerant of traditional antibiotic treatments[22].

The observation that heme is seemingly unimportant for the rate at which Bfr is able to oxidise and mineralise iron[23] led to the proposal that the ferroxidase centres and hemes function as two independent cofactors involved in iron uptake and iron release, respectively. Under oxidative stress or iron-replete conditions the Bfr ferroxidase centre couples oxidation of Fe^{2+} to the reduction of an external electron acceptor, most likely peroxide[24], performing the dual roles of consuming ROS and converting the potentially toxic Fe^{2+} into a chemically inert ferric mineral solubilized within the protein coat. Under low-iron conditions the heme cycles oxidation state by

accepting electrons from reduced Bfd and passing them to the mineral core, mobilising the iron by reducing it to Fe^{2+}, leading to release into the cytoplasm[20].

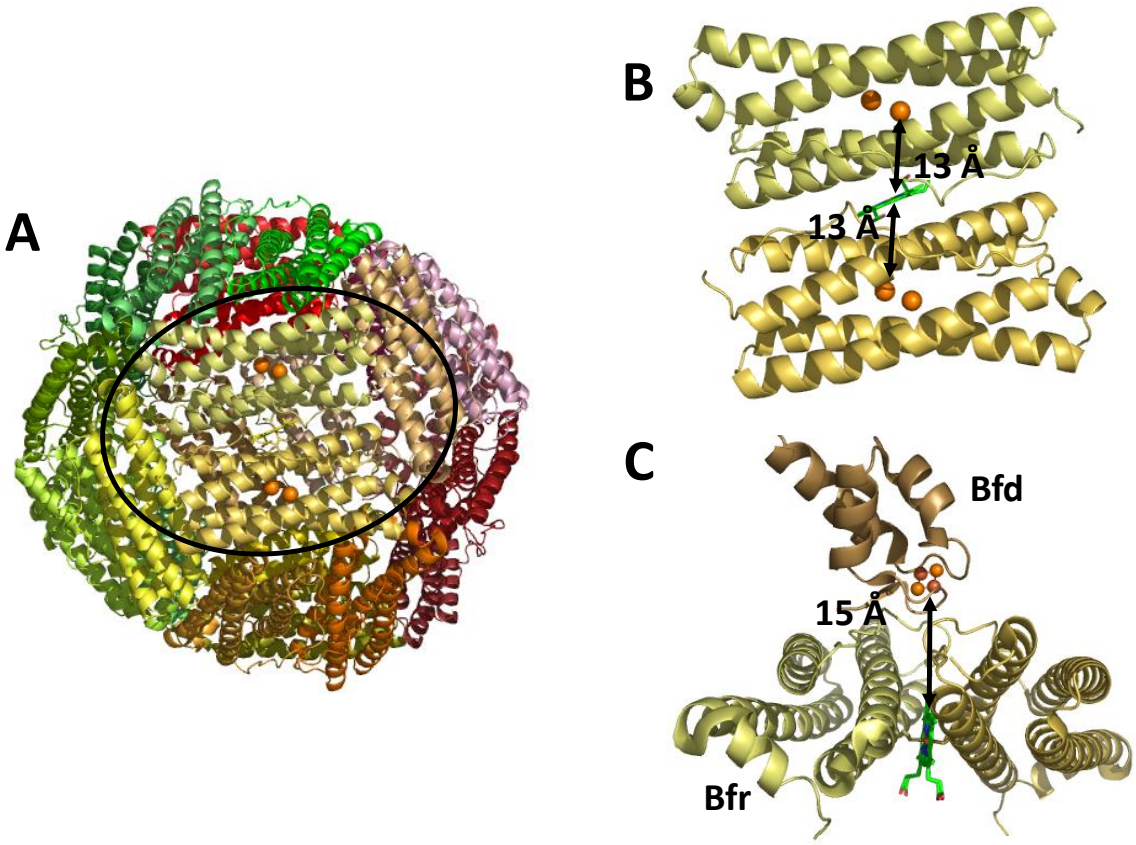

Figure 1. The structure of Bfr and its complex with Bfd. (A) Bfr monomers fold into a 4 α–helical bundle that spontaneously assemble to form a cage with rhombic dodecahedral symmetry composed of 24 identical subunits. Each face is made up of a dimer (one such face is highlighted by the black oval) in which the subunits are arranged anti-parallel to one another. (B) Each Bfr subunit contains a diiron site, the ferroxidase centre (orange spheres), and there is one heme site (in green) per dimer. The heme iron is separated from the nearest non-heme iron of the ferroxidase centre by approximately 13 Å. (C) Bfd binds to the outer surface of the cage directly above the heme such that the iron-sulfur cluster of the ferredoxin is approximately 15 Å from the edge of the porphyrin of the heme.

Unexpectedly, rapid electron transfer between heme and ferroxidase centre was recently demonstrated for the Bfr from *E. coli*, suggesting that the two cofactors may function in a connected way[25]. Here we employ a combination of absorbance, circular dichroism (CD) and magnetic circular dichroism (MCD) spectroscopies to investigate electron transfer between the hemes and ferroxidase centres of *E. coli* Bfr, and *in vitro* iron release assays that probe the effects of disabling the ferroxidase centres on the mobilisation of stored iron. The data demonstrate that, under conditions that promote release of iron from Bfr, the ferroxidase centres also act as a route of electron transfer into the mineral core.

Results and Discussion

Electron transfer from [2Fe-2S] Bfd to the hemes of Bfr drives iron core reduction and release. The reported midpoint potential of the [2Fe-2S] cluster of *E. coli* Bfd is ~-250 mV[26], higher than that of the candidate electron sources for iron release via reduction of the mineral core ($NADH/NAD^+$ and $NADPH/NADP^+$ at approximately at approximately -280 mV and -370 mV, respectively [27]. We therefore sought to exploit the complementary optical properties of iron-sulfur clusters and hemes to establish whether reduction of Bfr hemes by Bfd is thermodynamically favourable or requires the driving force of coupling to the more reducing nucleotides. Bfd from *P. aeruginosa* has been reported to reduce the heme of its cognate Bfr, but this conclusion was based solely on the position of the absorbance maximum of the Soret peak of the heme against a background of other contributing chromophores[20]. The inherent chirality of the Bfd cluster results in significant CD associated with the charge transfer bands of the oxidised form. In contrast, the near planarity of the Bfr heme results in negligible CD intensity but the large orbital angular momenta of the electronic excited states of the porphyrin mean that a longitudinal magnetic field induces a large dichroism and this MCD response is diagnostic of the oxidation state of the iron at the centre of the porphyrin[28]. Therefore recording of the CD and MCD spectra of mixtures of Bfr and Bfd allow the oxidation state of each cofactor to be deduced from spectra in which interfering contributions from the other are absent.

As reported for the *P. aeruginosa* protein[20], reduction of the Bfd $[2Fe\text{-}2S]^{2+}$ cluster by sub-stoichiometric addition of sodium dithionite resulted in bleaching of the ligand to metal charge transfer bands with consequent loss in CD intensity at 550 nm and a change in sign of the CD at around 460 nm (Fig. S1). The MCD of heme-reconstituted *E. coli* Bfr is characteritic of low spin ferric heme with an intense derivative feature centred on 420 nm and a weaker negative feature with a minimum at 577 nm. Incubation with one equivalent of reduced ($[2Fe\text{-}2S]^{1+}$) Bfd per heme resulted in a slight red shift of the derivative feature at low wavelength to 421 nm and the appearance of a sharp derivative feature centred on 564 nm, both indicative of the presence of low spin ferrous heme. Addition of excess reduced Bfd resulted in a further shift of the low wavelength feature to 423 nm and increased intensity of the sharp derivative, saturating at 3 equivalents of reduced Bfd per heme (Fig. 2A). Comparison of the intensity of the derivative feature at 564 nm to that of Bfr in which the heme was fully reduced by sodium dithionite indicated that incubation with excess reduced Bfd resulted in reduction of only ~33% of the heme. Consistent with this, the CD spectra (Fig. 2B) demonstrated incomplete oxidation of the clusters of the added Bfd, suggesting that the system reached equilibrium with both Bfd and Bfr partially reduced, but with the majority of hemes remaining oxidized, placing the midpoint potential of the Fe^{3+}/Fe^{2+} couple of the Bfr heme below that of the Bfd cluster.

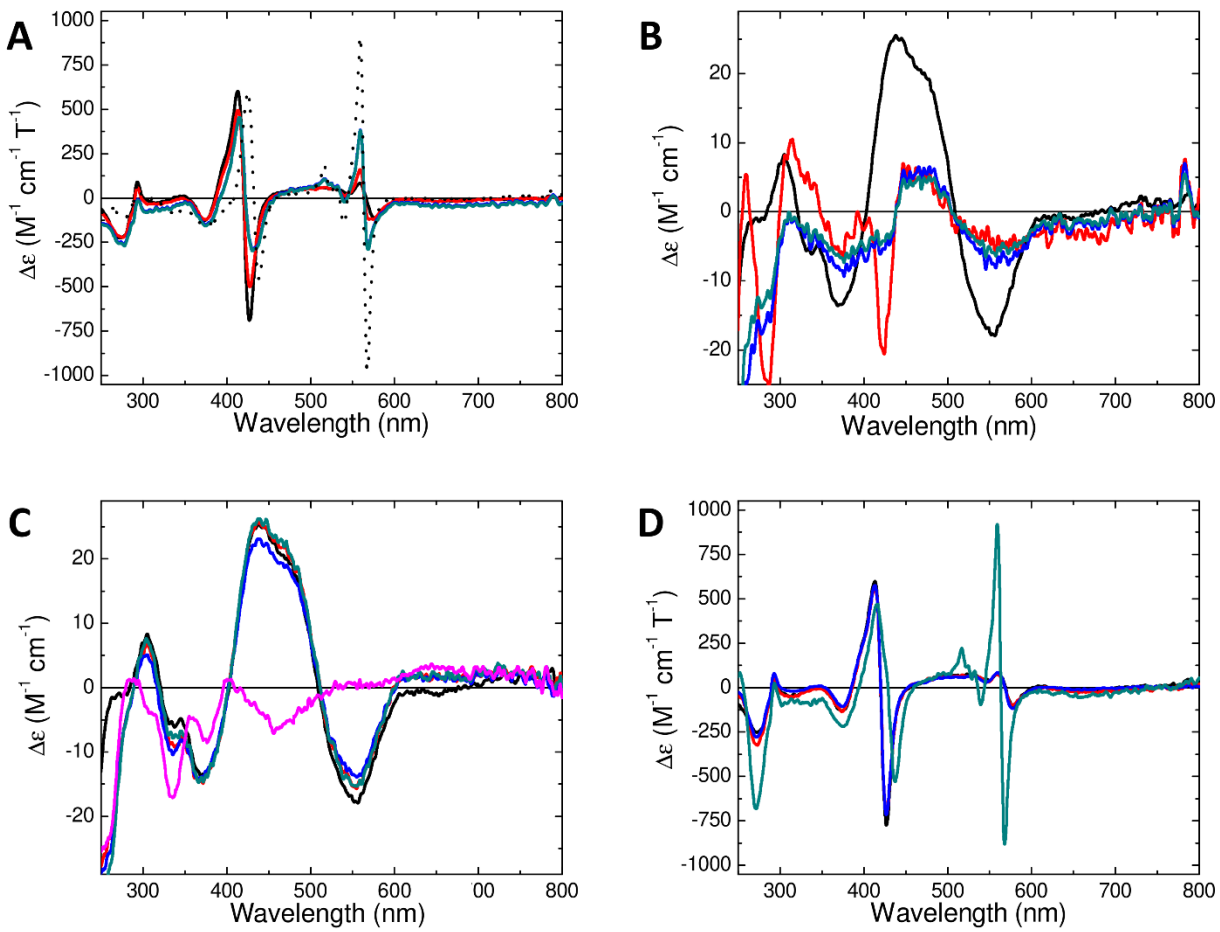

Figure 2. Electron transfer between NADH, NADPH, Bfd and Bfr. (A) The MCD spectra of heme-loaded Bfr (solid black trace), Bfr incubated with one equivalent of reduced Bfd per heme (red), 3 equivalents of reduced Bfd per heme (blue), 4 equivalents of reduced Bfd (teal) and excess sodium dithionite (dotted black trace). (B) The CD spectrum of oxidized Bfd (black) together with those of the Bfr/Bfd mixtures from (A). (C) The CD spectra of oxidized Bfd (black), and Bfd incubated with 4 equivalents of NADH (red), 4 equivalents of NADH and 0.2 units of FdR (blue), 4 equivalents of NADPH (teal) and 4 equivalents of NADPH and 0.2 units of FdR (purple). (D) The MCD spectra of heme loaded Bfr (black), Bfr incubated with 2 equivalents of NADH per heme (red), 2 equivalents of NADPH per heme (blue) and 0.5 equivalents of Bfd per heme in the presence of 0.2 units of FdR and excess NADPH (teal).

Early reports of the midpoint potential of the Fe^{3+}/Fe^{2+} couple in ferritin mineral cores place this well below the reported value of the Bfd cluster[29]. Given the apparent paradox of electron transfer from Bfd to both Bfr heme and mineral core being thermodynamically unfavourable, we sought to determine the effect of coupling the Bfd clusters to the greater reducing power of reduced dinucleotides. The cognate reductase for *E. coli* Bfd has yet to be identified so the commercially available NADPH-dependent ferredoxin reductase (FdR) from spinach was employed to facilitate electron transfer. Incubation with a 3-fold excess of reduced nucleotide had no effect on the CD spectrum of Bfd (Fig. 2C), indicating that the oxidation state of the ferredoxin

cluster was unchanged and hence that direct electron transfer did not occur. However, addition of 0.2 units of FdR led to complete reduction of Bfd clusters by NADPH.

In an experiment equivalent to that above but with NADH in place of NADPH, only 15% reduction over the course of 30 minutes was observed, demonstrating the requirement for a reductase to enable efficient electron transfer to the ferredoxin cluster. The model for Bfd-mediated iron release from Bfr, therefore, predicts that incubation of ferritin containing oxidized heme with Bfd, FdR and reduced nucleotide would lead to heme reduction in the case of NADPH but not NADH. Indeed, incubation of Bfr with excess NADPH but substoichiometric Bfd led to complete heme reduction on addition of FdR, whilst NADH had little effect on Bfr oxidation state under identical conditions (Fig. 2D). We therefore conclude that the Bfd cluster undergoes cycling of oxidation state under these conditions such that, in the presence of Bfr containing a mineral core, the NADPH/FdR/Bfd system would drive catalytic reduction of the encapsulated ferric mineral leading to release of the stored iron. Complete reduction of Bfr hemes by NADPH places the midpoint potential of the Fe^{3+}/Fe^{2+} couple at not less than –300 mV whilst the partial reduction observed on incubation with Bfd alone suggests a midpoint potential of not greater than –265 mV; thus the reduction potential of Bfr heme, E_m, lies between –300 and –265 mV at pH 6.5.

Attempts to detect release of Fe^{2+} from Bfr by monitoring the increase with time of absorbance at 563 nm due to the Fe^{2+}-ferrozine complex following addition of NADPH to an assay mixture containing FdR and Bfd were unsuccessful. Following an initial increase indicating chelation of Fe^{2+} the absorbance quickly plateaued. One possibility is that the [2Fe-2S] cluster of Bfd may be unstable in the presence of ferrozine due to the extraction of Fe^{2+}. Therefore, assays equivalent to those above were performed, except that ferrozine was added at defined timepoints after addition of NADPH and the instantaneous increase in 563 nm absorbance was recorded. This resulted in a clear linear increase in A563 nm, and hence concentration of released Fe^{2+}, over 30 minutes, such that approximately 10% of the stored iron was released over this period (Fig. 3). When Bfr samples that had not been reconstituted with heme following purification, or were loaded with zinc protoporphyrin IX in place of heme, were employed in equivalent iron-release assays, no such evidence of iron release driven by electron transfer from NADPH was observed.

We therefore conclude that the [2Fe-2S] cluster of Bfd is required to deliver electrons from NADPH to the Bfr heme, such that heme-deficient Bfr is unable to accept electrons from Bfd at a rate that leads to detectable release of Fe^{2+} in the assay employed here. Filling of vacant heme sites with zinc protoporphyrin IX also did not lead to measureable iron release, demonstrating that the presence of the porphyrin alone is not sufficient to support electron transfer into the interior of Bfr; a redox active metal at the centre of the macrocycle is required.

FMN drives Bfd-independent but heme-dependent iron release from Bfr. The data presented above demonstrated the ability of the Bfd cluster to cycle oxidation state in order to channel electrons from NADPH, via a ferredoxin reductase, into the heme of Bfr to drive release of Fe^{2+} from the interior of the ferritin. However, given the suspected fragility of the Bfd cluster towards ferrozine-induced loss of Fe^{2+}, an alternative heme reductant was sought in order to further investigate electron transfer events between the cofactors of Bfr and their implications for the mechanism of Fe^{2+} release.

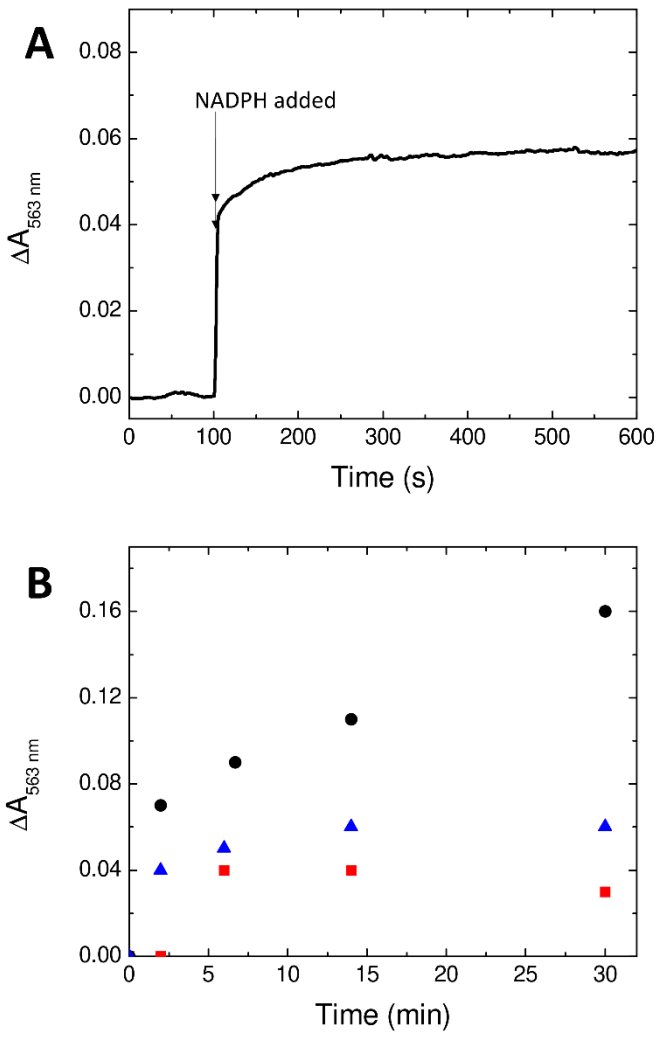

Figure 3. NADPH-driven iron release from Bfr. (A) Increase in 563 nm absorbance as a function of time following the addition of NADPH to a solution of iron-loaded Bfr containing 9 hemes per cage in the presence of 1 equivalent of Bfd per heme, 0.5 units of FdR and 1 mM ferrozine. (B) Instantaneous increase in 563 nm absorbance on addition of ferrozine to a solution of NADPH, Bfd, 0.5 units of FdR and iron-loaded Bfr containing either 9 hemes per cage (black circles), 1 heme per cage as present following purification (red squares) or 1 heme and 8 Zn Protoporphyrin IX per cage (blue triangles) as a function of incubation time with the NADPH.

FMN was explored as a possible candidate as it has been reported to drive the reductive release of iron from other ferritins[30] and removes the possibility of iron abstracted from the Bfd cofacor being misinterpreted as iron release from the Bfr mineral core. The riboflavin was reduced by anaerobic titration with a dithionite solution and the concentration of reducing equivalents calculated from the loss in intensity of the 446 nm absorbance feature (Fig. S2). Assays using 100 μM reduced FMN as the electron source revealed faster kinetics of Fe^{2+} release than those employing NADPH to reduce Bfd, most likely due to rate-limiting reduction of the ferredoxin by the non-cognate reductase in the latter case. However, comparison of the rate and extent of Fe^{2+} release from samples in which the majority of heme-binding sites were vacant with those in which

the site had been reconstituted with either heme or zinc protoporphyrin IX demonstrated that the most important route of electron transfer into the mineral core remained via the redox cycling of the heme iron (Fig. 4). Approximately 75% of mineralized iron was released from heme-loaded samples, decreasing to approximately 35% in those loaded with zinc protoporphyrin IX, compared to 40% in the protein as isolated. This suggests FMN passes electrons directly to the heme iron, in a manner not observed for either NADH or NADPH. This was confirmed to be the case for Bfr lacking any mineralised iron within the internal cavity (Fig. 5A).

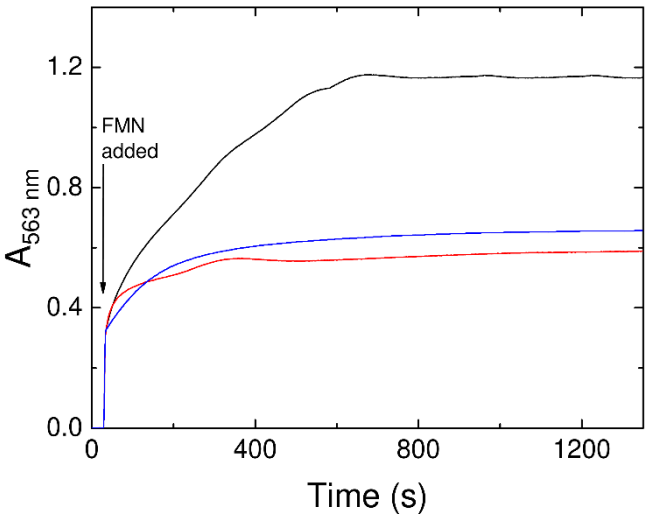

Figure 4. FMN-driven iron release from Bfr. Increase in 563 nm absorbance as a function of time following the addition of 100 μM FMN to solutions containing ferrozine and iron-loaded Bfr reconstituted with 9 hemes per cage (black), reconstituted with 8 Zn Protoporphyrin IX per cage (red) or with no reconstitution of vacant heme sites (blue).

The heme of Bfr is oxidized by di-Fe^{3+} ferroxidase centres. The recent report of oxidation of Bfr heme during ferroxidase centre turnover demonstrated the existance of a rapid electron transfer pathway between the two cofactors[25]. The midpoint potential for reduction of the diiron catalytic centre is significantly greater than that of the Met/Met ligated heme, as evidenced by the significant reduction of the former on incubation with a 1 mM solution of sodium ascorbate (E_m = +60 mV[31], Fig. S3). Taken together these observations suggest that the heme of Bfr should be spontaneously oxidized by Fe^{3+} bound to ferroxidase centre sites without need for external electron acceptors such as O_2 or peroxide.

This was investigated by utilising MCD to monitor the oxidation state of Bfr heme during titration with reduced FMN. A sample of Bfr reconstituted with heme was split into two aliquots. The first was incubated aerobically with 48 equivalents of Fe^{2+} in order to populate all ferroxidase centre sites with Fe^{3+} before equilibrating the sample with a N_2 atmosphere. The other was incubated anaerobically with 1 mM sodium ascorbate and 48 equivalents of Zn^{2+}, a potent inhibitor of ferroxidase centre activity that acts by preventing Fe^{2+} binding, and buffer exchanged by centrifugation to remove excess ascorbate and any unbound Zn^{2+}.

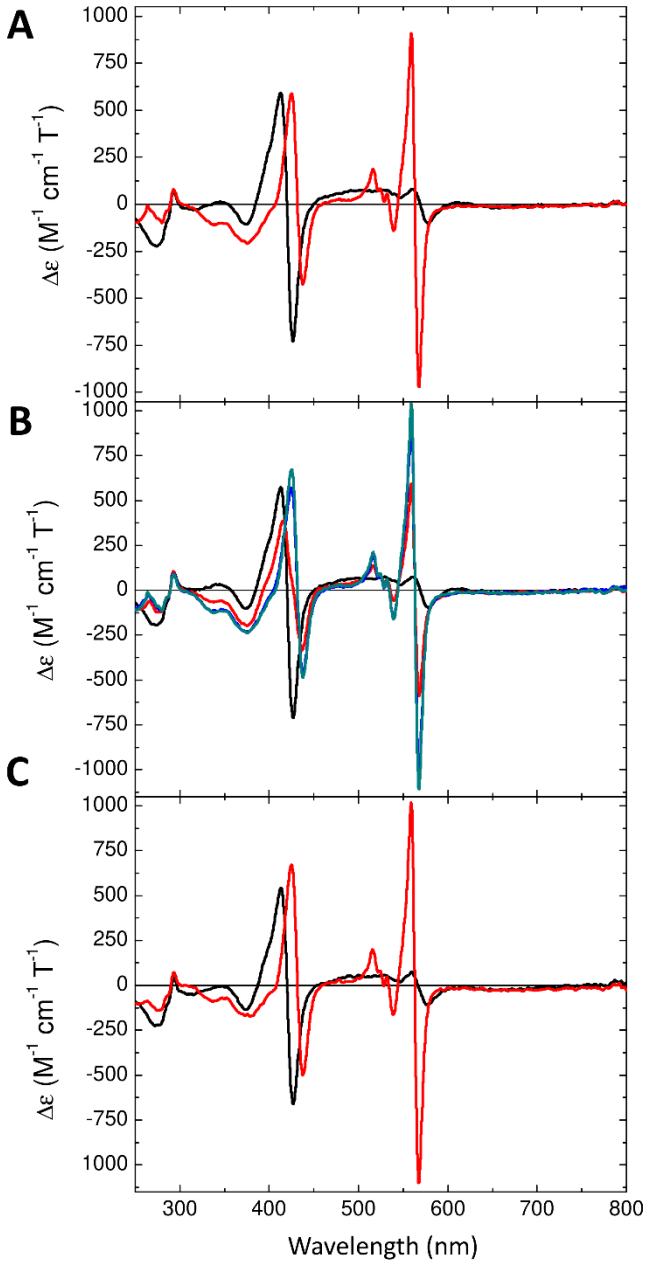

Figure 5. Reduction of Bfr hemes by FMN. (A) The MCD spectra of heme-loaded Bfr (black) and heme-loaded Bfr anaerobically incubated with 4 equivalents of FMN per protomer (red). (B) The MCD spectra of heme-loaded Bfr incubated aerobically with 2 equivalents of Fe^{2+} per protomer (black) prior to anaerobic incubation with 2 equivalents of FMN (red), 3 equivalents of FMN (blue) or 4 equivalents of FMN (teal) per protomer. (C) The MCD spectra of heme-loaded Bfr anaerobically incubated with 1 mm ascorbate and 2 equivalents of Zn^{2+} per protomer (black) prior to anaerobic incubation with 1 equivalent of FMN per protomer (red).

Bfr in which the ferroxidase centre sites were fully occupied with Fe^{3+} required 3 reducing equivalents of FMN per protomer in order to fully reduce the heme (Fig. 5B). In contrast, the heme of Bfr in which the ferroxidase centre has been rendered redox inactive by the binding of Zn^{2+} was

fully reduced following the addition of 1 reducing equivalent of FMN per protomer (Fig. 5C). Therefore FMN must either directly reduce the ferroxidase centres of Bfr in preference to the heme, or rapid electron transfer from reduced heme to oxidised ferroxidase centre occurs in the absence of O_2 or H_2O_2 as electron acceptors. Direct reduction of Fe^{3+} bound at the ferroxidase centre was discounted based on data from iron-release assays detailed below.

Ferroxidase centre-mediated iron release requires reduction via the heme. Loading of Bfr with zinc protoporphrin IX in place of heme resulted in significant impairment of the extent of iron release driven by FMN as reductant (Fig. 4). However approximately 35% of the stored iron was still chelated by ferrozine, raising the possibility that Fe^{3+} bound at ferroxidase centres is also able to mobilise some of the mineralized iron by acting as a conduit for electrons supplied from FMN.

The possible role of the ferroxidase centre in reductive mobilisation of the mineral core was probed by assaying the iron-release activity of Bfr with the diiron site inactivated. A control experiment in which Bfr loaded with 1200 equivalents of iron was anaerobically incubated with ascorbate and ferrozine confirmed that ascorbate only reduced iron at the ferroxidase centre and did not cause significant leeching of the mineral core (Fig. S4). Bfr preloaded with 9 heme and 1200 equivalents of Fe^{3+} was exposed to 48 equivalents of Zn^{2+} in the presence of 1 mM sodium ascorbate in order to inactivate the ferroxidase centres before buffer exchanging to remove reductant and any unbound Zn^{2+} or displaced Fe^{2+}. Exposure of this sample to 100 μM FMN as reductant resulted in Fe^{2+} release that was intermediate in extent between that of heme-loaded and zinc protoporphyrin IX-loaded Bfr, with approximately 55% of stored iron released 20 minutes after the addition of reduced FMN (Fig. 6A), indicating that inhibition of the ferroxidase centres significantly affected iron release.

Treatment equivalent to that above of a sample of Zn-Bfr loaded with 8 zinc protoporphyrin IX and 1200 Fe, such that both the majority of heme-binding and ferroxidase centre sites were rendered redox inactive, led to iron-release properties almost identical to those of Bfr containing zinc protoporphyrin IX in place of heme but with functioning ferroxidase centres (Fig. 6A). The data demonstrate that the ferroxidase centres contribute to the mobilisation of the Bfr mineral core, but that this contribution is dependent on the presence of heme. Thus, the ferroxidase centres are unable to accept electrons directly from FMN, but do so via the heme groups, resulting in subsequent transfer to the Fe^{3+} stored within the interior of the protein. Around 20% of the iron internalised within Bfr cages was released almost immediately upon addition of reduced FMN, regardless of heme loading or status of the ferroxidase centres. This, together with the observation of FMN-driven iron release from ferritins that do not bind heme suggests that this reductant is able to pass electrons through the protein coat, rapidly reducing a subpopulation of the mineralised iron. The nature of this iron subpopulation is currently unclear. We note that the rapid and uncontrolled release of iron mediated by FMN is not compatible with the requirement for controlled cellular iron metabolism.

Data equivalent to the above, generated using 100 μM reduced Bfd in place of FMN, confirmed the importance of the ferroxidase centre in iron release driven by the biologically relevant reductant. Ferrozine was added to assay solutions at defined time points following initiation of iron release by the addition of reduced Bfd to samples of Bfr preloaded with 1200 equivalents of Fe^{3+}. The instantaneous increase in absorbance at 563 nm as a function of time between the Bfd and ferrozine additions is shown in Fig. 6B. The pattern of behaviour was similar

to that observed in continuous assays utilising FMN as the electron source, with the greatest rate and extent of iron release (approximately 90% of total stored iron, complete in 3 minutes) observed for heme-loaded protein with active ferroxidase centres. Using Zn to inhibit the ferroxidase centres of heme-loaded Bfr reduced both the rate and extent of iron release with approximately 70% of mineralised iron released following 10 minutes incubation with reduced Bfd. As with FMN, the greatest effect was observed when the majority of heme binding sites were either vacant or contained Zn protoprphyrin IX, resulting in 50% of mineralised iron released in 10 minutes. Again, the effects of disabling the two cofactors were not cumulative: the iron release activity of Zn protoporphyrin IX-loaded Bfr in which the ferroxidase centres were disabled with Zn did not differ significantly from that in which the diiron site remains active, highlighting the importance of electron transfer from the hemes to the ferroxidase centres during iron release.

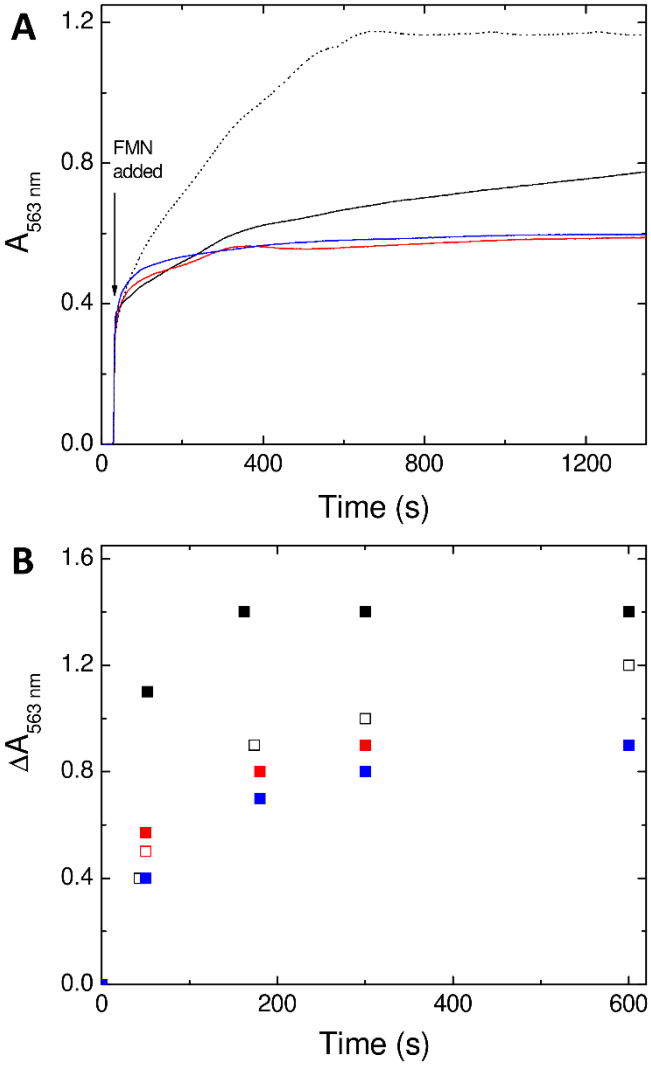

Figure 6. Effect of ferroxidase centre inhibition on iron release from Bfr. Increase in 563 nm absorbance as a function of time following the addition of 100 μM FMN to solutions containing ferrozine and iron-loaded Bfr reconstituted with 9 hemes per cage in which the ferroxidase centres had been inactivated by Zn^{2+} binding (black) and an equivalent sample reconstituted with 8 Zn protoporphyrin IX per cage in place of heme (blue). Red trace depicts the response of a sample reconstituted with 8 Zn

protoporphyrin IX per cage in which the ferroxidase centres remained active, and the broken black trace that of a sample reconstituted with 9 hemes per cage in which ferroxidase centres remained active. (B) Instantaneous increase in 563 nm absorbance upon addition of 1 mM ferrozine to Bfr pre-loaded with 1200 equivalents of iron as a function of time following addition of 100 μM reduced Bfd. Black data points represent Bfr reconstituted with 9 hemes per cage, red data points Bfr reconstituted with 8 Zn protoporphyrin IX per cage and blue data points Bfr in which the heme-binding site were not reconstituted following purification. Filled symbols represent Bfr with active ferroxidase centres and open black or red symbols Bfr in which ferroxidase centres were inactivated with Zn^{2+}. Note, for Zn protoporphyrin IX-reconstituted Bfr, the open and filled data points overlay at later time points.

Conclusions

Like all H-chain-type ferritins, Bfr contains an intra-subunit di-iron ferroxidase centre. Unlike all other ferritins it also contains another iron-containing cofactor in the form of heme located at inter-subunit sites (Fig. 1). These two cofactors are respectively required for the efficient oxidation of Fe^{2+} leading to iron mineralisation[32] and efficient reduction of Fe^{3+} in the mineral core leading to iron release back to the cytosol[19, 33]. For the latter process, the structure of Bfr in complex with Bfd revealed that the cluster of the ferredoxin is ideally situated to transfer electrons to the heme of the ferritin and this was demonstrated to form a conduit for electron transfer into the mineral core[20].

A recent report described rapid oxidation of Bfr heme on populating the ferroxidase centre with iron under aerobic conditions. The rate of heme oxidation was dependent on O_2 concentration suggesting rapid electron transfer between the two cofactors and that they may, in fact, be functionally connected[25]. Indeed, it has been reported that the heme of Bfr plays a minor role in iron mineralization at high iron loadings[34] and, although the basis of this was not known, electron transfer between the cofactors could account for such an effect. The midpoint potentials of the two cofactors suggest that electron transfer from heme to Fe^{3+} at the ferroxidase centre should be spontaneous without need for O_2 or H_2O_2 to act as an electron acceptor, and this was confirmed by reductive titrations reported here. Bfd, the physiologically relevant reductant for the heme, is not expressed under conditions where iron is sequestered by Bfr. It is therefore unlikely that the Bfr hemes would be reduced during iron uptake. It was previously proposed that electron transfer from the heme to the ferroxidase centre during iron release might enable Bfr to retain H_2O_2 detoxification capacity through its reaction at di-Fe^{2+} ferroxidase centres, even during iron release[25]. However, until now, a role for the ferroxidase centre in iron release has not been envisaged. The data presented here demonstrate that electron transfer from the heme to the ferroxidase centre is indeed important in mediating iron release.

The assays of FMN- and Bfd-driven iron release presented here demonstrate that inactivation of the ferroxidase centre results in a significant decrease in the rate and extent of recovery of internalised mineral, indicating a role for the diiron site in core reduction. This is consistent with the existence of an electron transfer pathway between iron bound on the inner surface of the protein and at the ferroxidase centre, postulated on the basis of the kinetics of Bfr-catalyzed Fe^{2+} oxidation[18a]. However Bfd and FMN are unable to directly reduce Fe^{3+} bound at the ferroxidase centre, with electrons instead transferred via transient reduction of the heme iron, consistent with the reported irreversible accumulation of iron in *P. aeruginosa* Bfr when heme reduction is prevented by disruption of the interaction with Bfd[21a, 22, 35]. We therefore propose that,

during release of mineralised iron from Bfr, the ferroxidase centres act as additional points of entry for electrons to the interior cavity. This would result in a greater proportion of stored iron being accessible to incoming electrons and hence a greater rate/extent of its recovery (Fig. 7).

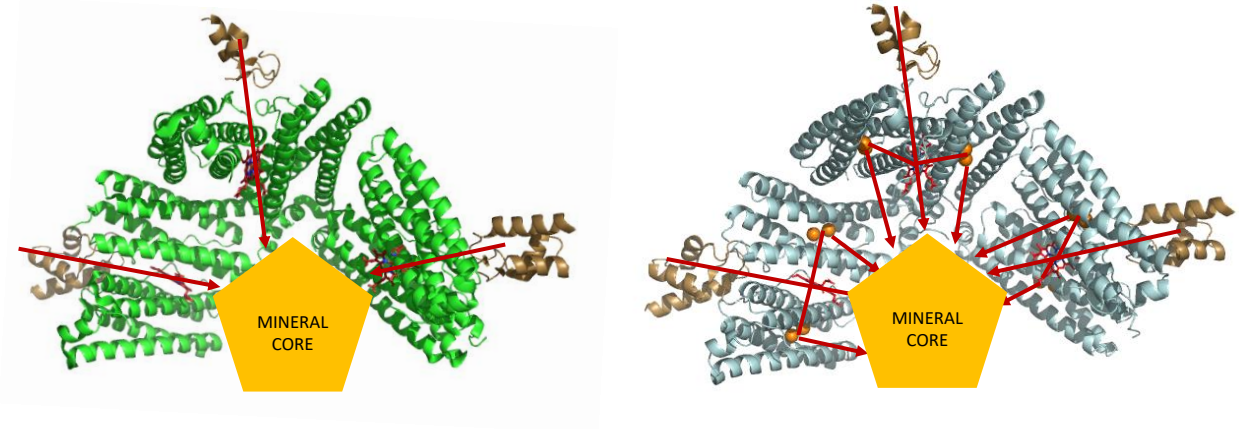

Figure 7. Reduction of the mineral core of Bfr. Schematic representation of a section of the Bfr cage with Bfd bound at the outer surface. The iron-sulfur cluster of Bfd provides a route for electrons to access the heme of Bfr. With the ferroxidase centres disabled, this constitutes the only route by which electrons can reach the mineral core (left). When ferroxidase centres are active these represent branching points in the electron transport chain, increasing the number of points of entry for electrons into the immobilised mineral, increasing the proportion of stored iron that can be recovered (right).

Ferroxidase centre-mediated reduction of mineralised iron may at first sight appear inconsistent with the irreversible accumulation of iron in the absence of Bfd binding[21a]. However, the midpoint potential of the mineral core very likely lies below that of iron bound at the ferroxidase centre, such that the diiron site is incapable of reducing the ferric mineral in the absence of the thermodynamic driving force of the reduced heme. This is consistent with the observation that ferroxidase centre reduction by 100 μM sodium ascorbate is unable to drive significant iron release *in vitro* (Fig. S4) and a midpoint potential for the Bfr mineral core below that of the +12 mV reported for ferrihydrite[36]. The extent of iron release driven by excess reduced Bfd suggest a midpoint potential for the core significantly more positive than the -300 to -400 mV reported from microcoulometry measurements[29]. However these estimates vary by 100 mV depending on choice of mediator to promote electron transfer, whilst the data presented here describe direct electron transfer between the species of interest without need for mediators.

This study demonstrates that Bfr hemes are directly reduced by FMN, possibly due to some affinity for the Bfd binding site placing it in close proximity, and that FMN appears capable of directly reducing (in an uncontrolled way) a subpopulation of the iron mineral. However, the majority of intracellular riboflavin is bound to the proteome (e.g. flavodoxins) with high (nM) affinity[37]. Therefore whilst the estimated intracellular concentration of FMN in *E. coli* is approximately 50 μM[38], that of free FMN is below 1 μM[39] and thus FMN is unlikely to be a physiologically relevant driver of iron release from Bfr. In the absence of Bfd and ferredoxin reductase, the nucleotides NADPH and NADH are unable to reduce the heme of Bfr, and neither is reduced glutathione (Fig. S5), suggesting that the low molecular weight reductants that are likely to be encountered *in vivo* would be incapable of driving reductive release of stored iron. This is supported by the absence of significant iron release *in vitro* for assays using either 100 μM

or 1 mM glutathione as reductant (Fig. S4). We therefore conclude that reduced Bfd represents the only viable source of electrons for the *in vivo* reduction of Bfr hemes, consistent with the reported consequences of disrupting this protein-protein interaction in *P. aeruginosa*[21a]. However, once reduced, the hemes of Bfr can either pass an electron directly into any mineral stored within the protein or do so via the ferroxidase centre, thereby increasing the proportion of stored iron accessible for rapid reductive mobilisation.

In summary, the literature on bacterioferritins indicates that the ferroxidase centre is required for iron oxidation/mineralisation, while the hemes are required for iron reduction/release. Recent data demonstrating electron transfer between the heme and ferroxidase centre of *E. coli* Bfr suggested that their functions may be coupled. Here, we demonstrate that the ferroxidase centre plays a previously unrecognised but crucial role in iron release, facilitated by electron transfer from Bfd via the heme. The impact of this is most likely to increase the points of entry of electrons into the central cavity for Fe^{3+} reduction and subsequent Fe^{2+} release.

Data Availability

All data are available from the corresponding author upon request.

Competing Interests

The authors declare that there are no competing interests associated with the manuscript.

Acknowledgements

Dr Myles Cheesman for access to the Circular Dichrograph and accompanying solid state magnet.

Funding

We thank UEA for supporting JMB's position, the award of a PhD studentship to ZB, and for the purchase of the solid state magnet.

Author Contributions

J.M.B.: conceptualization, investigation, formal analysis, writing – original draft. **Z.B.:** investigation, formal analysis, writing – review and editing. **A.S.:** investigation, formal analysis; **S.C.A.:** investigation, writing – review and editing; **M.T.W**.: writing – review and editing; **D.A.S.:** writing – review and editing; **G.R.M.:** writing – review and editing. **N.L.B.:** conceptualization, funding acquisition, supervision, writing – review and editing.

Abbreviations

Bfr, bacterioferritin; EDTA, ethylene diamine tetraacetic acid; HEPES 4-(2-hydroxy ethyl)-1-piperazine ethanesulfonic acid; LB, lysogeny broth; MES, 2-(N-morpholino) ethanesulfonic acid;

Tris, tris(hydroxymethyl)aminoethane; SDS, sodium dodecyl sulfonate; PAGE, poly acrylamide gel electrophoresis.

References

[1] S. Hedrich, M. Schlomann, D. B. Johnson, *Microbiology* **2011**, *157*, 1551-1564.
[2] F. W. Outten, E. C. Theil, *Antioxid. Redox. Sig.* **2009**, *11*, 1029-1046.
[3] D. Touati, *Arch. Biochem. Biophys.* **2000**, *373*, 1-6.
[4] J. M. Bradley, D. A. Svistunenko, M. T. Wilson, A. M. Hemmings, G. R. Moore, N. E. Le Brun, *J. Biol. Chem.* **2020**, *295*, 17602-17623.
[5] E. C. Theil, M. Matzapetakis, X. F. Liu, *J. Biol. Inorg. Chem.* **2006**, *11*, 803-810.
[6] X. F. Liu, E. C. Theil, *Acc. Chem. Res.* **2005**, *38*, 167-175.
[7] R. R. Crichton, J. P. Declercq, *Biochim. Biophys. Acta* **2010**, *1800*, 706-718.
[8] A. Ilari, S. Stefanini, E. Chiancone, D. Tsernoglou, *Nat. Struct. Biol.* **2000**, *7*, 38-43.
[9] J. M. Bradley, G. R. Moore, N. E. Le Brun, *Curr. Opin. Chem. Biol.* **2017**, *37*, 122-128.
[10] P. Arosio, T. G. Adelman, J. W. Drysdale, *J. Biol. Chem.* **1978**, *253*, 4451-4458.
[11] D. M. Lawson, A. Treffry, P. J. Artymiuk, P. M. Harrison, S. J. Yewdall, A. Luzzago, G. Cesareni, S. Levi, P. Arosio, *FEBS Lett.* **1989**, *254*, 207-210.
[12] S. Ciambellotti, C. Pozzi, S. Mangani, P. Turano, *Chem. Eur. J.* **2020**, *26*, 5770-5773.
[13] A. Dautant, J. B. Meyer, J. Yariv, G. Precigoux, R. M. Sweet, A. J. Kalb, F. Frolow, *Acta Crystallogr. D* **1998**, *54*, 16-24.
[14] M. R. Cheesman, A. J. Thomson, C. Greenwood, G. R. Moore, F. Kadir, *Nature* **1990**, *346*, 771-773.
[15] H. L. Yao, A. Soldano, L. Fontenot, F. Donnarumma, S. Lovell, J. R. Chandler, M. Rivera, *Biomolecules* **2022**, *12*, 366.
[16] J. M. Bradley, G. R. Moore, N. E. Le Brun, *J. Biol. Inorg. Chem.* **2014**, *19*, 775-785.
[17] S. K. Weeratunga, S. Lovell, H. L. Yao, K. P. Battaile, C. J. Fischer, C. E. Gee, M. Rivera, *Biochemistry* **2010**, *49*, 1160-1175.
[18] a) J. M. Bradley, D. A. Svistunenko, T. L. Lawson, A. M. Hemmings, G. R. Moore, N. E. Le Brun, *Angew Chem Int Edit* **2015**, *54*, 14763-14767; b) A. Crow, T. L. Lawson, A. Lewin, G. R. Moore, N. E. Le Brun, *J. Am. Chem. Soc.* **2009**, *131*, 6808-6813.
[19] S. Yasmin, S. C. Andrews, G. R. Moore, N. E. Le Brun, *J. Biol. Chem.* **2011**, *286*, 3473-3483.
[20] H. L. Yao, Y. Wang, S. Lovell, R. Kumar, A. M. Ruvinsky, K. P. Battaile, I. A. Vakser, M. Rivera, *J. Am. Chem. Soc.* **2012**, *134*, 13470-13481.
[21] a) K. Eshelman, H. L. Yao, A. Hewage, J. J. Deay, J. R. Chandler, M. Rivera, *Metallomics* **2017**, *9*, 646-659; b) A. Hewage, L. Fontenot, J. Guidry, T. Weldeghiorghis, A. K. Mehta, F. Donnarumma, M. Rivera, *Pathogens* **2020**, *9*, 980.
[22] A. Soldano, H. L. Yao, A. Hewage, K. Meraz, J. K. Annor-Gyamfi, R. A. Bunce, K. P. Battaile, S. Lovell, M. Rivera, *ACS Infect. Dis.* **2021**, *7*, 123-140.
[23] S. C. Andrews, N. E. Le Brun, V. Barynin, A. J. Thomson, G. R. Moore, J. R. Guest, P. M. Harrison, *J. Biol. Chem.* **1995**, *270*, 23268-23274.
[24] J. Pullin, M. T. Wilson, M. Clemancey, G. Blondin, J. M. Bradley, G. R. Moore, N. E. Le Brun, M. Lucic, J. A. R. Worrall, D. A. Svistunenko, *Angew. Chem. Int. Ed.* **2021**, *60*, 8361-8369.
[25] J. Pullin, J. M. Bradley, G. R. Moore, N. E. Le Brun, M. T. Wilson, D. A. Svistunenko, *Angew. Chem. Int. Ed.* **2021**, *60*, 8376-8379.
[26] M. A. Quail, P. Jordan, J. M. Grogan, J. N. Butt, M. Lutz, A. J. Thomson, S. C. Andrews, J. R. Guest, *Biochem. Biophy, Res. Commun.* **1996**, *229*, 635-642.
[27] H. Huang, S. Wang, J. Moll, R. K. Thauer, *J. Bacteriol.* **2012**, *194*, 3689-3699.

[28] M. R. Cheesman, C. Greenwood, A. J. Thomson, *Adv. Inorg. Chem.* **1991**, *36*, 201-255.
[29] N. D. Chasteen, I. M. Ritchie, J. Webb, *Anal. Biochem.* **1991**, *195*, 296-302.
[30] a) T. Jones, R. Spencer, C. Walsh, *Biochemistry* **1978**, *17*, 4011-4017; b) S. Sirivech, E. Frieden, S. Osaki, *Biochem. J.* **1974**, *143*, 311-315; c) D. L. Jacobs, G. D. Watt, R. B. Frankel, G. C. Papaefthymiou, *Biochemistry* **1989**, *28*, 1650-1655; d) W. L. Jin, H. Takagi, B. Pancorbo, E. C. Theil, *Biochemistry* **2001**, *40*, 7525-7532.
[31] L. P. Jenner, J. M. Kurth, S. van Helmont, K. P. Sokol, E. Reisner, C. Dahl, J. M. Bradley, J. N. Butt, M. R. Cheesman, *J. Biol. Chem.* **2019**, *294*, 18002-18014.
[32] S. Baaghil, A. Lewin, G. R. Moore, N. E. Le Brun, *Biochemistry* **2003**, *42*, 14047-14056.
[33] a) A. Mohanty, A. Parida, B. Subhadarshanee, N. Behera, T. Subudhi, P. K. Koochana, R. K. Behera, *Inorg. Chem.* **2021**, *60*, 16937-16952; b) M. Rivera, *Acc. Chem. Res.* **2017**, *50*, 331-340.
[34] S. G. Wong, R. Abdulqadir, N. E. Le Brun, G. R. Moore, A. G. Mauk, *Biochem. J.* **2012**, *444*, 553-560.
[35] A. Soldano, H. L. Yao, J. R. Chandler, M. Rivera, *ACS Infect. Dis.* **2020**, *6*, 447-458.
[36] M. Aeppli, R. Kaegi, R. Kretzschmar, A. Voegelin, T. B. Hofstetter, M. Sander, *Environ. Sci. Technol.* **2019**, *53*, 3568-3578.
[37] A. C. Wilson, A. B. Pardee, *J. Gen. Microbiol.* **1962**, *28*, 283-303.
[38] J. O. Park, S. A. Rubin, Y. F. Xu, D. Amador-Noguez, J. Fan, T. Shlomi, J. D. Rabinowitz, *Nat. Chem. Biol.* **2016**, *12*, 482-489.
[39] P. J. Holt, R. G. Efremov, E. Nakamaru-Ogiso, L. A. Sazanov, *Biochim. Biophys. Acta* **2016**, *1857*, 1777-1785.